NanoMaterialsCAD: Flexible Software for the Design of Nanostructures

Giorgos Nikoulis, Panagiotis Grammatikopoulos, Stephan Steinhauer[1], Joseph Kioseoglou*

G. Nikoulis, Prof. J. Kioseoglou

Department of Physics, Aristotle University of Thessaloniki, GR-54124 Thessaloniki, Greece

Dr. P. Grammatikopoulos, Dr. S. Steinhauer

Okinawa Institute of Science and Technology Graduate University, 1919-1 Tancha, Onna-Son, Okinawa 904-0495 Japan

E-mail: sifisl@auth.gr

Keywords: CAD, software, GUI, nanoparticles, nanostructures

Abstract

NanoMaterialsCAD is a new open source tool dedicated to the creation, manipulation, and 3D visualization of crystalline structures at the nanoscale. It is designed for pre-processing atomistic configurations to be used as input for atomistic (e.g., molecular dynamics or Monte Carlo) or *ab initio* (e.g., density functional theory) computer simulations. It offers several tools for designing complex nanostructures (including nanoparticles, nanowires, nanotubes, nanoscrolls, etc., and combinations/permutations of them) which are either lacking or cumbersome in other existing packages. Through its intuitive graphical user interface (GUI) it enables facile ways to design and modify the

---

[1] Current address: Department of Applied Physics, KTH Royal Institute of Technology, SE 106-91, Stockholm, Sweden

size/shape and relative positions of nanoobjects while observing the changes in real time. NanoMaterialsCAD is written in C++, and exploits OpenGL (for the GUI), Win32API (for interaction with Windows), and Assembly (for fast data management). The source code and executable file are available for download from GitHub. We aspire that NanoMaterialsCAD will be adopted by the nanomaterials modeling community as a valuable resource; to this end we will keep improving it, incorporating more nanostructures and adding extra functionalities to its toolbox.

1. Introduction

Computer simulation is a powerful tool for elucidating the electronic or atomistic nature of various phenomena at the nanoscale. With rapid advances in computer capacity and algorithms, and the rise of High Performance Computing (HPC), little doubt remains that the prominence of computational nanoscience is also constantly increasing. Indeed, a recent literature search showed that more than 7,000 articles on nanomaterials simulations are currently indexed in Web of Science per year, more than double than just ten years ago. [1] This rapid surge is also attributed to the advances in experimental methodologies regarding the fabrication and application of nanoparticles, thin films, and other nanostructures, simultaneously leading to a demand for more in-depth theoretical analysis. [2] [3] [4] [5] [6] [7] [8] As a result, one of the main challenges for computational nanoscience is to design increasingly sophisticated simulation models that correspond accurately to real-life systems and the conditions in experimental setups. [9] [10] [11] [12] [13] [14] [15] [16]

A crucial aspect of this challenge is the creation of the desired initial nanostructures, an often tedious and time-consuming task which sometimes proves harder than anticipated. Especially when the configuration is complicated and its physical properties are sensitively dependent on structure, small misjudgments on, e.g., nanoparticle facet orientations or nanotube dimensions can yield misleading or, indeed, wrong

results. Currently, several programs are available for modeling and visualizing atomistic systems, such as OVITO, [17] ATOMS, [18] and VESTA. [19] Although all of them offer valuable tools for manipulating a system, and a graphical user interface (GUI) for the user to interact with, there are specific tasks that these programs cannot perform (at least, to date), which are important for certain studies, e.g., creating a nanotube or a nanoscroll, inserting random point defects, introducing random displacements of atoms, creating big databases of systems, etc. Commercial packages also exist, such as Materials Studio Visualizer, [20] but, as such, are not freely available to everyone.

Our previous experience with performing computer simulations that complement experimental work on NP design and utility in various nanodevices [21] [22] [23] [24] [25] has revealed the need for software that enables facile nanostructure design. Of particular significance has been the demand to reproduce surfaces and interfaces obtained from microscopy characterization of experimental samples, because of their importance in the determination of, e.g., electronic structures and chemical, magnetic, or plasmonic properties, etc. [21] [22] [26] [27] [28] With this work, we are introducing our newly developed software, NanoMaterialsCAD, [29] which caters for such needs. It is a free tool for modeling and manipulation of nanoobjects at the atomic level that provides an easy and automated way to create various kinds of crystalline structures such as nanoparticles, nanodots, nanowires, nanotubes, nanoscrolls, spatial vacuums, etc., all packed into a single integrated application. This paper covers the basics of our software's capabilities; others are discussed in our Supplementary Information document containing a users' manual. Our aspiration is that NanoMaterialsCAD will be adopted by the nanomaterials modeling community as a valuable resource; to this end we will keep improving it, incorporating more nanostructures and adding extra functionalities to its toolbox.

2. Software Description

NanoMaterialsCAD [29] is an open source tool dedicated to the creation and manipulation of crystalline structures at the nanoscale. One of its strongest aspects is that it offers easy and intuitive ways to change

the shape and/or the size of nanoobjects in real time while observing the changes immediately. This enables quick and straightforward initialization of structures to be used in first-principle or atomistic simulations of various methods. Especially in certain studies where the ability to create a big number of system replicas with minor variations (e.g., to create training sets for Machine Intelligence generated interatomic potentials) is crucial, NanoMaterialsCAD offers an efficient solution: the user can write their own scripts and execute them by calling them from inside the program. A `FOR` loop in the script can be used to create a great number of structures, which, combined with the ability of the program to generate randomized configurations, can lead to numerous variations of the system.

2.1. General Information

The source code is implemented with C++, exploiting object-oriented programming, and OpenGL for the graphical interface. NanoMaterialsCAD offers an optimized GUI for the user to interact with (**Figure 1**a), as well as multiple additional tools that can help manipulate it. Some of them are (i) unit cell multiplication to create super cells, (ii) rotation and translation of selected atoms, (iii) real-time distance calculation between any pair of atoms even while modifying their relevant positions, (iv) interactive surface manipulation, (v) randomization of system properties, etc. The user can also insert random or hand-picked vacancies, randomize the initial position of atoms by small displacements, randomize the initially defined occupancy of crystal atomic positions (e.g., to create atomistic supercells for high entropy alloys), etc.

Some of these operations can be used by calling commands in the command line, a fast way to access certain utilities of the program. Further, Win32API allows the use of a dropdown menu with various options (Figure 1b), enables drag-and-drop for input files, handles the communication between the user and the program through the Windows Procedure, and creates a command window as a child window, thus making the overall interface more user-friendly. Some parts of the program are written in Assembly for more efficient data management. With fast performance being top priority, two modes are available

4

for rendering atoms: points and spheres. Using spheres, one can readily render 10,000 atoms running at 60 fps (using Intel i5 CPU, 4th gen. 3.20 GHz). Using point rendering, however, similar performance can be achieved for ten times more atoms.

To appeal to a broad user base, the program is currently compatible with VASP[30] and LAMMPS,[31] two of the most widely used simulation packages, and can handle any POSCAR file (a prototype file invented and used by the VASP team to describe crystalline structures) as input and produce POSCAR or LAMMPS files as output. Using a POSCAR file as input for a given unit cell, a crystalline structure can be generated either by using the command line or by selecting a "*mold*" from the menu (corresponding to various structures available), also using the `supercell` command to multiply the unit cell and create an extended nanocrystal. The GUI lists the facets of the molds on the top-left corner of the window, along with indication of where the facets intersect the *x*, *y*, and *z* axes (in Å). For a cubic system this indicates the distance of each facet from the center of the structure, whereas for a hexagonal system it indicates the distance from the mid-point of the edges. Atom type and number are indicated on the right side of the window (Figure 1a). Various functions can be performed using the mouse, mouse wheel, and selected keys.

Next, we are going to analyze program utilities and offer some examples and case studies to demonstrate the usage of the software. For more information on software usage the reader may refer to Supplementary Information document and real-time video which serve as an up-to-date instruction manual as of the submission date of this manuscript; however, as NanoMaterialsCAD will be under constant development, more updated versions may be found online.

2.2 Design of 0D structures

NanoMaterialsCAD provides an easy way to create symmetrical nanoparticles (NPs). In the *Edit* tab of the top bar menu (Figure 1b) three options (*Cubic*, *Hexagonal*, and *Sphere*) create NPs with specific

surfaces which can be subsequently modified by the user (i.e., surface ratios and/or NP size can be changed). The structure is updated in real time so the user can immediately inspect the changes while being applied to the system.

Let us use a Cr unit cell to demonstrate the creation of various exemplary NPs. First, we drag-and-drop the POSCAR file that contains the unit cell; then we pick the *Cubic* option from the *Edit* menu tab. Using the command `supercell(10,10,10)` we create a crystal box containing 10×10×10 repetitions of the unit cell, maintaining its bcc symmetry. The NP is then ready for the user to modify its surfaces and change their ratios or the NP size altogether. The origin of the axes is also redefined by the command `supercell(x,y,z)`, which duplicates the system and creates a *x* by *y* by *z* system. Initially the system is a 1×1×1 unit cell, which means that the origin of the axes is simply the vertex (0,0,0) of the simulation box. Once we use the command `supercell(x,y,z)` we duplicate the whole system, which means we also duplicate the (0,0,0) vertex. The algorithm finds the duplicated vertex closest to the center of the system and sets it as the new origin of the axes. This allows the NP to be in the center of the simulation box and, thus, easier to observe.

For the *Cubic* option the surface families are the {100}, {110}, and {111} of the cubic system. Each facet is represented by a plane equation:

$$Ax + By + Cz + D = 0 \qquad (1)$$

where *A*, *B*, and *C* are constants for each facet defining the orientation of the surface. *D* is the parameter that the user can modify. Keys that allow surface manipulation are "*q*" and "*w*", "*a*" and "*s*", and "*z*" and "*x*": each key moves a specific family of surfaces closer to or farther from the center of the NP. In doing so, the initially cubic NP morphs smoothly into NPs of other shapes (**Figure 2**), enabling to explore the full configurational space of symmetric Cr NPs. The importance of such a possibility will become clear through case study 1, below. The same can be done for a NP with a hexagonal symmetry by picking the *Hexagonal* mold option, whereas spherical NPs are easily produced with the *Sphere* mold, with the user defining the radius.

2.3. Design of 1D Structures

NanoMaterialsCAD is capable of creating 1D structures such as nanowires (NWs), nanorods (NRs), nanoscrolls (NSs), and nanotubes (NTs); this is the focus of this section.

NWs and NRs can be created in two ways. The first is through the *Rod-like* option from the *Edit* tab in the program menu (Figure 1b). This option works as those discussed for NPs in the previous section, only this time the user eliminates the termination of the nanocrystal upon specific surfaces, thus extending the nanorods along specific directions (see Supplementary Information for details). The user can manipulate the surfaces again with the "*q*", "*w*", "*a*", "*s*", "*z*" and "*x*" keys. The second way is by specifying the exact surfaces; here is an example of creating a simple, infinitely long NW from the command line:

```
cut(1,0,0,10)

cut(-1,0,0,10)

cut(0,1,0,10)

cut(0,-1,0,10)
```

creating a NW of (100), ($\bar{1}$00), (010), and (0$\bar{1}$0) surfaces at a distance of 10 Å from its central axis. Commands will be covered in more detail in a following section.

For NSs and NTs, on the other hand, the program requires a 2D material to help construct the structure. By inserting the 2D material in the program and navigating to *Edit → Nanoscroll* (Figure 1b), the algorithm constructs a NS from the initial 2D structure by rolling it around the *x*-axis according to the Archimedean spiral equation (see Appendix A for details). The inner and outer radii lengths of the NS can be adjusted with the "*q*" and "*w*" and the "*a*" and "*s*" keys. One can create a NT by matching the values of the two radii (shown on the top-left corner of the window).

2.4. Design of 2D Structures

2D materials may be of interest by themselves, or required to construct NSs or NTs. Typical examples include carbon sheets, transition metal dichalcogenides, and hydrogen-terminated thin films. A simple way to create 2D materials is by slicing from a corresponding bulk system:

```
supercell(40,40,20)

cut(0,0,1,5)

cut(0,0,-1,5)
```

This exemplary sequence of commands first creates an atomistic supercell of 40×40×20 crystal lattice parameters and then cuts a 2D slice 10 Å in thickness along the *z* direction.

2.5. Custom structure design

All systems discussed until now possess some form of symmetry which makes them easy to construct in an automated fashion; for example, the NPs in Figure 2 are symmetric with respect to their center, NTs have axial symmetry, and so on. Such systems are useful as model systems, showcasing basic principles. However, oftentimes in real-life experiments more complex and/or defected nanostructures appear that deviate significantly from an ideal system, which need to be accurately reproduced and simulated. This is the focus of this section.

The command line is a tool designed to give the user freedom in designing complex structures (a text predictor is also included for easy use). It also operates when a mold is enabled: for example, if the spherical mold is selected, the user can cut the spherical NP wherever they want while working with it. Some basic options available through the command line will be discussed here; for more details, or for more commands, the interested reader can refer to Supplementary Information.

The command `cut(h,k,l,D)` that was used in previous sections cuts the system along the plane (hkl). The fourth variable, D, is the one that appears in the plane equation (1). In practice, if we consider equation (1) explicitly, e.g., the command `cut(1,2,3,6)` in a cubic system provides a plane which intersects the x-axis at 6 Å, the y-axis at 3 Å, and the z-axis at 2 Å. This way the user is not limited to a given set of planes but they can create any combination of surfaces at will. The command `cut(h,k,l,D)` limits a 3D crystal within a given plane, as described by the Miller indices. For example, `cut(-1,2,0,20)` applies the $(\bar{1},2,0)$ plane and cuts the axis at the 20 Å mark. For hexagonal systems the same command can be used omitting the third plane component. For example, if a_1, a_2, a_3, a_4 are the axes of a hexagonal system, where $a_1=x$ and $a_4=z$, the command `cut(1,0,0,10)` cuts the a_1 axis at 10 Å and the a_3 at -10 Å.

One can also select specific atoms and either delete them, thus adding random or hand-made vacancies, or replace them with atoms of a different type, which can play an important role on the material's thermodynamical, mechanical, or optical properties. To replace atoms the user has to right-click on the screen and navigate to *Edit Selected → Change Element*; a window then appears in which they can choose any element. This feature can be very useful for, e.g., terminating surfaces with hydrogen atoms (**Figure 3**a).

Of course, the user may combine any given number of individual nanoobjects to recreate an experimentally observed structure. By inverting the `IF` statements used to construct any nanoobject the user can also create a void within the volume or on the surface of a crystal. This way one can, for example, half-embed a nanoparticle in an underlying support, as shown in Figure 3b. A case study of an asymmetric Pt NP on a CuO substrate, as observed through high resolution transmission electron microscopy (HRTEM), is discussed in case study 2, below.

3. Case Studies

Next, we will cover two case studies where simulations were performed on systems designed with NanoMaterialsCAD. The goal is to demonstrate our new tool's comparative advantage with respect to other currently available software. Also, to highlight its flexibility, the first case study concerns classical molecular dynamics (MD) simulations performed with LAMMPS, whereas the second is a density functional theory (DFT) investigation performed with VASP. As mentioned above, both codes are among the most commonly used for their respective methods, thus indicating the potential widespread utility of our new software tool.

3.1 Case study 1: Determination of equilibrium shapes of Fe NPs with MD

Prediction of NP shapes is key to various nanotechnology applications since efficiency often depends heavily on shape. Catalysis is an obvious example, with dissimilar NP morphologies offering different numbers of active sites for reactions. [32] [33] [34] [35] Equilibrium NP shapes are typically determined from Wulff constructions and surface energy minimization arguments; therefore, one would intuitively expect spherical (or near-spherical) shapes to occur, i.e., NPs with the lowest possible surface-to-volume ratios. [36] [37] [38] [39] [40] [41] [42] [43] However, in real-life experiments non-spherical geometries often prevail, driven by either thermodynamic or kinetic effects. [28] [44] [45]

A useful benchmarking practice in determining the probability of specific NP shapes for given sizes is to identify the thermodynamically stable shape and calculate its differences in energy compared with those of other shapes. [46] For example, Zhao et al. recently explained the formation of Fe nanocubes grown by magnetron-sputtering inert-gas condensation based on differences in kinetic growth modes of different-type facets (namely, {100} and {110}). [44] To do so, the authors first compared the potential energy (as a function of NP size) for five different shapes (i.e., cube; edge-cut cube; sphere; truncated rhombic dodecahedron, TRD; and rhombic dodecahedron, RD), and concluded that, within the studied size range, the TRD was consistently the most stable structure. However, it should be mentioned that only a TRD with equilateral hexagon facets and a specific edge-cut cube were included in that assessment; this

10

sufficed for that study, as the main conclusion from that comparison was that nanocubes were clearly energetically unfavorable and, therefore, their existence could not be explained by thermodynamics arguments. If, on the other hand, one needed to perform a more rigorous comparison, including all possible chamfered cube shapes for any given NP size, one would have to face the tedious and time-consuming task of generating all these intermediate initial structures.

NanoMaterialsCAD offers the possibility to generate these structures efficiently and effortlessly, using the procedure described above. We thus created nanocubes ranging between 1 and 8 nm in edge length, and morphed them by edge chamfering toward edge-cut cubes, TRD, and, eventually, RD NPs. In doing so, we varied the ratio between total areas of {100} and {110} facets, starting with purely {100}-terminated cubes and ending with purely {110}-terminated RD. Obviously, the number of intermediate shapes increased as the NP size increased, as indicated by the number of points in **Figure 4**a. In this figure the potential energy per atom is plotted as a function of NP size, calculated by molecular statics simulations performed with LAMMPS using the EAM potential developed by Mendelev et al. (as in Zhao et al.). [47] A zoom-in at the chamfering sequence for the 8 nm cubes is shown in the Figure 4b, indicating that the energetically favorable structure is not the equilateral TRD, but a chamfered cube (also describable as a non-equilateral TRD) with a surface area ratio of $\frac{A_{110}}{A_{100}} = 1.075$. A visual aid in obtaining energetically optimal structures is shown in Figure 4c. A comparison of potential energies of three NP shapes (sphere, cube, and non-equilateral TRD) is shown in Figure 4d, along with equivalent results from Zhao et al. We notice that there is good agreement between the two studies, with the TRD being the energetically favorable shape followed by the sphere and the cube. The slightly lower values obtained consistently in the current work are a result of performing the study at 0K, instead of room temperature as in the previous work, which reduced the potential energy by ~0.04eV/atom and are not of essence; what is of interest is the relative trends for each individual study. In particular, our goal here was to produce a very detailed plot based on a great number of initial structures generated by NanoMaterialsCAD, which can prove useful for future studies. Further, NanoMaterialsCAD can be a very useful tool in evaluating

the transferability of an interatomic potential (which are often fitted to bulk properties) to the nano-regime, by comparing its prediction with the Wulff constructions of nanoparticles of given sizes.

3.2 Case study 2: Calculation of charge transfer between asymmetrical Pt NP and CuO support with DFT

Surface charge and charge transfer between metallic NPs and metal-oxide supports are of great importance for various applications in catalysis, surface plasmonics, electrochemistry, etc. [26] [27] [48] Especially in the field of chemical (bio-) sensing, the nature of the NP-oxide support interface and the resulting interactions can determine the sensitivity and selectivity of the sensor device. [49] [50] [51] *Ab initio* theoretical studies based on real-life experimental data are often necessary to characterize these interfaces accurately. To this end, HRTEM is a valuable tool, providing detailed information with atomic resolution on real systems.

Our second case study demonstrates the practical usefulness of NanoMaterialsCAD in readily translating HRTEM data into accurately reproduced structures to be used in DFT calculations. As a model system we used a Pt NP deposited on CuO support, as shown in **Figure 5**a. CuO nanowires were grown by thermal oxidation of Cu [52] and were decorated with Pt NPs by magnetron sputtering inert-gas condensation. [3] Pt NPs are well-known to exhibit superior catalytic activity, owing to the effective electron transfer from the NPs to the supports, especially reducible oxides such as cupric oxide. [53] [54] [55] Here, the main challenges in reproducing this exemplary structure were the asymmetry of the NP and the relative orientation of its crystal structure with respect to the support.

To recreate this particular NP, after drag-and-dropping the relevant POSCAR file, we followed the process described above for NRs: we first created a $10 \times 10 \times 10$ Å^3 supercell, and then cut the bulk system along the corresponding surfaces indicated by the HRTEM micrograph. We notice that this particular NP

is terminated only by surfaces of the {111} family (figure 5a, inset). To construct the substrate, we drag-and-dropped the CuO unit cell [56] and created a 1×1×2 super cell. By doing so, we created four layers of CuO along the [111] direction. The bottom layer had to be passivated with a pseudo-hydrogen layer for subsequent DFT simulations. [57] To create the pseudo-hydrogen atoms we defined *Change Element* as "*H1.5*" so that hydrogen atoms possess 1.5 electron charges each. After saving the file (*ctrl+s*), we opened it in a text editor and added a 15 Å vacuum along the [111] direction; we could then relax the system with VASP to find the optimal positions for the Cu, O, and pseudo-H atoms. After the relaxation finished we opened the output CONTCAR file with the NanoMaterialsCAD and multiplied it with `supercell(5,4,1)` to create a 4×5 surface onto which the Pt NP was deposited.

Both the NP and the substrate files could be rendered in the same scene (to select individual files, one can left-click on the plus sign at the top-left corner and click on the desired file). After composing the full structure, we selected the NP alone and translated / rotated it (by right-clicking and selecting *Translate* or *Rotate*, respectively, from the *Edit → Selected* tab). The distance of the NP from the substrate was also controlled with the distance calculator tool, located at the left toolbar (if one atom from the NP and one atom from the support are selected, their distance is instantly updated while moving the NP). Therefore, NanoMaterialsCAD provided a facile way to precisely place the NP on top of the substrate as necessary to reproduce the experimental configuration.

Once the desired configuration was achieved, we used DFT modeling to investigate the charge transfer mechanism. The methodology is described in detail in the Supplementary Information and in references [26] [27]. Figure 5b shows a charge density transfer plot of the system, that is, a projection on the *x-z* plane of the total charge density difference between the overall structure (i.e., the relaxed Pt NP resting on the CuO NW) and its corresponding isolated constituents (i.e., the relaxed Pt NP and the bare CuO NW surface). Pronounced electron charge transfer is observed at the interfacial area, mainly caused by the highly electronegative O atoms bonding with the Pt atoms of the NP. [27] Polarization and charge separation also occurred in the volume of the NP and the CuO; this is more visible in the CuO where the polarity

13

of the polar covalent bonds between Cu and O changes. The increased strong electric dipoles located on Pt atoms close to the interfacial area evidently increase the positive charges of Pt atoms. The charge density transfer plot of Figure 5b clearly shows that a cloud of electrons is located beneath the Pt NP, which consequently leads to positively charged upper layers of the CuO NW. Our results highlight the electronic NP-support interactions in the Pt-CuO system, which is relevant for the correct interpretation of experimental studies. Hence, this example showcases how NanoMaterialsCAD can aid in the efficient design of computational models to understand the structure-property relations and functionalities of hybrid nanomaterials.

4. Conclusion and prospects for future expansion

In this paper we introduced NanoMaterialsCAD, an open source manipulation and visualization tool dedicated to the creation of crystalline structures. We covered structures such as NPs, NWs, NSs, NTs, 2D materials, and more. We also explained the usage of the command line and introduced various utility commands that assist in the manipulation of the system. Two case studies were presented that demonstrate the usability of the program. In the former, we smoothly morphed Fe NPs from cubic through chamfered-cubic and to, eventually, RD shapes, thus exploring their full configurational space; we also calculated their configurational energies by classical MD. In the latter, we accurately reproduced a configuration of a single Pt NP deposited on a CuO substrate (observed experimentally by HR-TEM), and investigated the electron charge transfer with DFT. For both case studies, we offered a step by step method of how to create the system with our software and explained the results of the simulation.

NanoMaterialsCAD is constantly under development. Near-future additions will include incorporation of amorphous and defect-based NPs. Algorithms will be considered for the parametric formation of twinned and multiply twinned NPs (such as decahedra and Mackay icosahedra), as well as possible other structures (such as anti-Mackay icosahedra, pentadodecahedra, polyicosahedra, Leary tetrahedra, etc.).

14

[58] [59] [60] As an open source resource, NanoMaterialsCAD will also benefit from users adding utilities and functionalities, and sharing plug-ins based on their own needs and priorities, thus expanding its scope.

Appendix A: Nanotubes and Nanoscrolls: *(Archimedean Spiral)*

To create a nanoscroll, a 2D layer is required as input, which is mapped onto a scroll of two given radii. Given a length, *S*, of this layer, the corresponding length of the nanoscroll is given by:

$$S(\theta) = \frac{r}{2\theta}\left(\theta\sqrt{1 + \theta^2} + ln\left(\theta + \sqrt{1 + \theta^2}\right)\right) (A1)$$

This expression is known as the *Archimedes' Spiral*. For simplicity we assume that the nanoscroll starts with $R = 0$ and ends up with $R = r$. If we solve this specific problem, it is trivial to generalize it and create a nanoscroll with inner radius $R = r_0$ and outer radius $R = r_1$.

For a given radius *r* and a given length $S(\theta)$, equation (A1) needs to be solved for θ. Since it is impossible to find an analytical solution for θ, we have to find the solution using a numerical method. We selected one open and one closed method, namely the bisection and Newton-Raphson methods. Both produced correct results, but the Newton-Raphson method proved superior in solving this specific problem. By following the Newton-Raphson method, we need to calculate the derivative $\frac{dS(\theta)}{d\theta}$, which is almost constant for $\theta \geq 5°$, at $\frac{dS(\theta)}{d\theta} \cong 0.5$, (for $\theta = 5°, \frac{dS(\theta)}{d\theta} = 0.47$) as it is shown in Figure A1.

This means that iterating only once using the Newton-Raphson method, we can find a solution of θ with very good precision, thus saving significant time.

15

Acknowledgements

Conflict of Interest

No conflict of interest has been declared by the authors.

References

[1]   K. Nordlund, "Perspective of computational modeling of nanomaterials," in *Computational Modelling of Nanomaterials*, Amsterdam, Elsevier, 2020, p. 244.

[2]   Y. Huttel, Gas-Phase Synthesis of Nanoparticles, Weinheim: Wiley-VCH, 2017.

[3]   P. Grammatikopoulos, S. Steinhauer, J. Vernieres, V. Singh and M. Sowwan, "Nanoparticle design by gas-phase synthesis," *Adv. Phys.: X,* vol. 1, no. 1, pp. 81-100, 2016.

[4]   D. Foster, T. Pavloudis, J. Kioseoglou and R. Palmer, "Atomic-resolution imaging of surface and core melting in individual size-selected Au nanoclusters on carbon," *Nat. Commun.,* vol. 10, p. 2583, 2019.

[5]   A. Bakin, J. Kioseoglou, B. Pecz, A. El-Shaer, A.-C. Mofor, J. Stoemenos and A. Waag, "Misfit reduction by a spinel layer formed during the epitaxial growth of ZnO on sapphire using a MgO buffer layer," *J. Cryst. Growth,* vol. 308, p. 314, 2007.

[6]   D. Nelli, G. Rossi, Z. Wang, R. Palmer and R. Ferrando, "Structure and orientation effects in the coalescence of Au clusters," *Nanoscale,* vol. 12, no. 14, pp. 7688-7699, 2020.

[7]   G. Förster, M. Benoit and J. Lam, "Alloy, Janus and core–shell nanoparticles: numerical modeling of their nucleation and growth in physical synthesis," *Physical Chemistry Chemical Physics,* vol. 21, no. 41, pp. 22774-22781, 2019.

[8] A. Ponchet, S. Combettes, P. Benzo, N. Tarrat, M. Casanove and M. Benoit, "Equilibrium shape of core (Fe)–shell (Au) nanoparticles as a function of the metals volume ratio," *Journal of Applied Physics,* vol. 128, no. 5, p. 055307, 2020.

[9] P. Grammatikopoulos, "Atomistic modeling of the nucleation and growth of pure and hybrid nanoparticles by cluster beam deposition," *Curr. Opin. Chem. Eng.,* vol. 23, p. 164, 2019.

[10] H. Seo, J. Park, J. Chang, K. Dae, M.-S. Noh, S.-S. Kim, C.-Y. Kang, K. Zhao, S. Kim and J. Yuk, "Strong stress-composition coupling in lithium alloy nanoparticles," *Nature Communications,* vol. 10, no. 1, p. 3428, 2019.

[11] Z. Zheng, H.-H. Wu, H. Liu, Q. Zhang, X. He, S. Yu, V. Petrova, J. Feng, R. Kostecki, P. Liu, D.-L. Peng, M. Liu and M.-S. Wang, "Achieving Fast and Durable Lithium Storage through Amorphous FeP Nanoparticles Encapsulated in Ultrathin 3D P-Doped Porous Carbon Nanosheets," *ACS nano,* vol. 14, no. 8, pp. 9545-9561, 2020.

[12] Q. He, B. Yu, Z. Li and Y. Zhao, "Density Functional Theory for Battery Materials," *Energy Environ. Mater,* vol. 2, no. 4, p. 264–279, 2019.

[13] D. Xue, P. Wang, Z. Zhang and Y. Wang, "Enhanced methane sensing property of flower-like SnO2 doped by Pt nanoparticles: A combined experimental and first-principle study," *Sensors and Actuators, B: Chemical,* vol. 296, p. 126710, 2019.

[14] Y. Lykhach, S. Kozlov, T. Skála, A. Tovt, V. Stetsovych, N. Tsud, F. Dvořák, V. Johánek, A. Neitzel, J. Mysliveček, S. Fabris, V. Matolín, K. Neyman and J. Libuda, "Counting electrons on supported nanoparticles," *Nature Materials,* vol. 15, no. 3, pp. 284-288, 2016.

[15] D. Kwak, M. Wang, K. Koski, L. Zhang, H. Sokol, R. Maric and Y. Lei, "Molybdenum Trioxide (α-MoO3) Nanoribbons for Ultrasensitive Ammonia (NH3) Gas Detection: Integrated Experimental and Density Functional Theory Simulation Studies," *ACS Appl. Mater. Interfaces,* vol. 11, no. 11, p. 10697–10706, 2019.

[16] V. Postica, A. Vahl, D. Santos-Carballal, T. Dankwort, L. Kienle, M. Hoppe, A. Cadi-Essadek, N. De Leeuw, M.-I. Terasa, R. Adelung, F. Faupel and O. Lupan, "Tuning ZnO Sensors Reactivity toward Volatile Organic Compounds via Ag Doping and Nanoparticle Functionalization," *ACS Appl. Mater. Interfaces,* vol. 11, no. 34, p. 31452–31466, 2019.

[17] A. Stukowski, "Visualization and Analysis of Atomistic Simulation Data with OVITO-the Open Visualization Tool," *Modelling Simul. Mater. Sci. Eng.,* vol. 18, p. 015012, 2010.

[18] "ATOMS," Shape software, [Online]. Available: http://www.shapesoftware.com/.

[19] K. Momma and F. Izumi, "VESTA: a three-dimensional visualization system for electronic and structural analysis," *J. Appl. Cryst.,* vol. 41, p. 653, 2008.

[20] "Biovia Materials Studio," [Online]. Available: https://www.gga.asia/upload/pdf/495/materials-

visualizer_20170927141318.pdf.

[21] M. Bohra, P. Grammatikopoulos, V. Singh, J. Zhao, E. Toulkeridou, S. Steinhauer, J. Kioseoglou, J.-F. Bobo, K. Nordlund, F. Djurabekova and M. Sowwan, "Tuning the onset of ferromagnetism in heterogeneous bimetallic nanoparticles by gas phase doping," *Phys. Rev. Mater.,* vol. 1, p. 066001, 2017.

[22] S. Steinhauer, J. Zhao, V. Singh, T. Pavloudis, J. Kioseoglou, K. Nordlund, F. Djurabekova, P. Grammatikopoulos and M. Sowwan, "Thermal oxidation of size-selected Pd nanoparticles supported on CuO nanowires: the role of the CuO-Pd interface," *Chem. Mater,* vol. 29, no. 14, p. 6153, 2017.

[23] A. Halder, J. Kioseoglou, B. Yang, K. L. Kolipaka, S. Seifert, J. Ilavsky, M. Pellin, M. Sowwan, P. Grammatikopoulos and S. Vajda, "Nanoassemblies of ultrasmall clusters with remarkable activity in carbon dioxide conversion to C1 fuels," *Nanoscale,* vol. 11, p. 4683, 2019.

[24] S. Kumar, T. Pavloudis, V. Singh, H. Nguyen, S. Steinhauer, C. Pursell, B. Clemens, J. Kioseoglou, P. Grammatikopoulos and M. Sowwan, "Hydrogen flux through size-selected Pd nanoparticles into underlying Mg nanofilms," *Adv. Energy Mater.,* vol. 8, p. 1701326, 2018.

[25] P. Grammatikopoulos, J. Kioseoglou, A. Galea, J. Vernieres, M. Benelmekki, R. E. Diaz and M. Sowwan, "Kinetic trapping through coalescence and the formation of patterned Ag-Cu nanoparticles," *Nanoscale,* vol. 8, p. 9780, 2016.

[26] A. J. Porkovich, Z. Ziadi, P. Kumar, J. Kioseoglou, N. Jian, L. Weng, S. Steinhauer, J. Vernieres, P. Grammatikopoulos and M. Sowwan, "In situ observation of metal to metal oxide progression: a study of charge transfer phenomenon at Ru-CuO interface," *ACS Nano,* vol. 13, no. 11, p. 12425, 2019.

[27] A. Datta, A. J. Porkovich, P. Kumar, G. Nikoulis, J. Kioseoglou, T. Sasaki, S. Steinhauer, P. Grammatikopoulos and M. Sowwan, "Single nanoparticle activities in ensemble: a study on Pd cluster nanoportals for electrochemical oxygen evolution reaction," *J. Phys. Chem. C,* vol. 123, p. 26124, 2019.

[28] J. Vernieres, S. Steinhauer, J. Zhao, A. Chapelle, P. Menini, N. Dufour, R. E. Diaz, K. Nordlund, F. Djurabekova, P. Grammatikopoulos and M. Sowwan, "Gas phase synthesis of multifunctional Fe-based nanocubes," *Adv. Funct. Mater.,* vol. 27, p. 1605328, 2017.

[29] G. Nikoulis, "github: NanoMaterialsCAD," [Online]. Available: https://github.com/cossphy/NanoMaterialsCAD.

[30] G. Kresse and J. Furthmüller, "Efficient iterative schemes for ab initio total-energy calculations using a plane-wave basis set," *Phys. Rev. B,* vol. 54, p. 11169, 1996.

[31] S. Plimpton, "Fast parallel algorithms for short-range molecular dynamics," *J. Comput. Phys.,* vol. 117, p. 1, 1995.

[32] S. Vajda and M. G. White, "Catalysis applications of size-selected cluster deposition," *ACS Catal.,* vol. 5, no. 12, p. 7152, 2015.

[33] Y. Lei, F. Mehmood, S. Lee, J. Greeley, B. Lee, S. Seifert, R. E. Winans, J. W. Elam, R. J. Meyer, P. C. Redfern, D. Teschner, R. Schlogl, M. J. Pellin, L. A. Curtiss and S. Vajda, "Increased silver activity for direct propylene epoxidation via subnanometer size effects," *Science,* vol. 328, p. 224, 2010.

[34] L. Cheng, C. Yin, F. Mehmood, B. Liu, J. Greeley, S. Lee, B. Lee, S. Seifert, R. E. Winans, D. Teschner, R. Schlogl, S. Vajda and L. A. Curtiss, "Reaction mechanism for direct propylene epoxidation by alumina-supported silver aggregates: the role of the particle/support interface," *ACS Catal.,* vol. 4, no. 1, p. 32, 2014.

[35] M. L. Eggersforfer, D. Kadau, H. J. Herrmann and S. E. Pratsinis, "Aggregate morphology evolution by sintering: number & diameter of primary particles," *J. Aerosol. Sci.,* vol. 46, p. 7, 2012.

[36] F. Baletto and R. Ferrando, "Structural properties of nanoclusters: energetic, thermodynamic, and kinetic effects," *Rev. Mod. Phys.,* vol. 77, p. 371, 2005.

[37] M. Jose-Yacaman, J. A. Ascencio, H. B. Liu and J. Gardea-Torresdey, "Structure, shape and stability of nanometric sized particles," *J. Vac. Sci. Technol. B,* vol. 19, p. 1091, 2001.

[38] K. Koga and K. Sugawara, "Population statistics of gold nanoparticle morphologies: direct determination by HREM observations," *Surf. Sci.,* vol. 529, p. 23, 2003.

[39] Z. Y. Li, N. P. Young, M. Di Vece, S. Palomba, R. E. Palmer, A. L. Bleloch, B. C. Curley, R. L. Johnston, J. Jiang and J. Yuan, "Three-dimensional atomic-scale structure of size-selected gold nanoclusters," *Nature,* vol. 451, p. 46, 2008.

[40] Z. W. Wang and R. E. Palmer, "Determination of the ground-state atomic structures of size-selected Au nanoclusters by electron-beam-induced transformations," *Phys. Rev. Lett.,* vol. 108, p. 245502, 2012.

[41] D. Reinhard, B. D. Hall, D. Ugarte and R. Monot, "Size-independent fcc-to-icosahedral structural transition in unsupported silver clusters: an electron diffraction study of clusters produced by inert-gas aggregation," *Phys. Rev. B,* vol. 55, p. 7868, 1997.

[42] D. Reinhard, B. D. Hall, P. Berthoud, S. Valkealahti and R. Monot, "Usupported nanometer-sized copper clusters studied by electron diffraction and molecular dynamics," *Phys. Rev. B,* vol. 58, p. 4917, 1998.

[43] J.-G. Mattei, P. Grammatikopoulos, J. Zhao, V. Singh, J. Vernieres, S. Steinhauer, A. Porkovich, E. Danielson, K. Nordlund, F. Djurabekova and M. Sowwan, "Gas-phase synthesis of trimetallic nanoparticles," *Chem. Mater.,* vol. 31, no. 6, p. 2151, 2019.

[44] J. Zhao, E. Baibuz, J. Vernieres, P. Grammatikopoulos, V. Jansson, M. Nagel, S. Steinhauer, M. Sowwan, A. Kuronen, K. Nordlund and F. Djurabekova, "Formation mechanism of iron nanocubes in

magnetron sputtering inert gas condensation," *ACS Nano,* vol. 10, no. 4, p. 4684, 2016.

[45] M. Zervos, C. Mihailescu, J. Giapintzakis, C. Luculescu, N. Florini, P. Komninou, J. Kioseoglou and A. Othonos, "Broad compositional tunability of indium tin oxide nanowires grown by the vapor-liquid-solid mechanism," *APL Mater.,* vol. 2, p. 056104, 2014.

[46] J. Vernieres, S. Steinhauer, J. Zhao, P. Grammatikopoulos, R. Ferrando, K. Nordlund, F. Djurabekova and M. Sowwan, "Site-specific wetting of iron nanocubes by gold atoms in gas-phase synthesis," *Adv. Sci.,* vol. 6, p. 1900447, 2019.

[47] M. I. Mendelev, S. Han, D. J. Srolovitz, G. J. Ackland, D. Y. Sun and M. Asta, "Development of new interatomic potentials appropriate for crystalline and liquid iron," *Philos. Mag.,* vol. 83, p. 3977, 2003.

[48] J. Scholl, A. García-Etxarri, A. Koh and J. Dionne, "Observation of quantum tunneling between two plasmonic nanoparticles," *Nano Letters,* vol. 13, no. 2, pp. 564-569, 2013.

[49] S. Steinhauer, J. Vernieres, J. Krainer, A. Kock, P. Grammatikopoulos and M. Sowwan, "In situ chemoresistive sensing in the environmental TEM: probing functional devices and their nanoscale morphology," *Nanoscale,* vol. 9, p. 7380, 2017.

[50] S. Steinhauer, V. Singh, C. Cassidy, C. Gspan, W. Grogger, M. Sowwan and A. Kock, "Single CuO nanowires decorated with size-selected Pd nanoparticles for CO sensing in humid atmosphere," *Nanotechnology,* vol. 26, p. 175502, 2015.

[51] E. Danielson, V. Dhamodharan, A. Porkovich, P. Kumar, N. Jian, Z. Ziadi, P. Grammatikopoulos, V. Sontakke, Y. Yokobayashi and M. Sowwan, "Gas-phase synthesis for label-free biosensors: zinc-oxide nanowires functionalized with gold nanoparticles," *Sci. Rep.,* vol. 9, p. 17370, 2019.

[52] S. Steinhauer, A. Chapelle, P. Menini and M. Sowwan, "Local CuO nanowire growth on microhotplates: in situ electrical measurements and gas sensing application," *ACS Sensors,* vol. 1, no. 5, p. 503, 2016.

[53] M. Mao, H. Lv, Y. Li, Y. Yang, M. Zeng, N. Li and X. Zhao, "Metal support interaction in Pt nanoparticles partially confined in the mesopores of microsized mesoporous CeO2 for highly efficient purification of volatile organic compounds," *ACS Catal.,* vol. 6, no. 1, p. 418, 2016.

[54] G. N. Vayssilov, Y. Lykhach, A. Migani, T. Staudt, G. P. Petrova, N. Tsud, T. Skala, A. Bruix, F. Illas, K. C. Prince, V. Matolin, K. M. Neyman and J. Libuda, "Support nanostructure boosts oxygen transfer to catalytically active platinum nanoparticles," *Nat. Mater.,* vol. 10, no. 4, p. 310, 2011.

[55] F. B. Ometto, E. A. Carbonio, E. Teixeira-Neto and H. M. Villulas, "Changes induced by transition metal oxides in Pt nanoparticles unveil the effects of electronic properties on oxygen reduction activity," *J. Mater. Chem. A,* vol. 7, no. 5, p. 2075, 2019.

[56] R. G. Wyckoff, Crystal Structures, New York: Interscience Publishers, 1963.

[57] Y. Zhang, J. Zhang, K. Tse, L. Wong, C. Chan, B. Deng and J. Zhu, "Pseudo-hydrogen passivation: a novel way to calculate absolute surface energy of zinc blende (111)/(111) surface," *Sci. Rep.,* vol. 6, p. 20055, 2016.

[58] R. Ferrando, Structure and properties of nanoalloys, Amsterdam: Elsevier, 2016.

[59] D. M. Foster, R. Ferrando and R. E. Palmer, "Experimental determination of the energy difference between competing isomers of deposited, size-selected gold nanoclusters," *Nature Communications,* vol. 9, p. 1323, 2018.

[60] D. Bochicchio and R. Ferrando, "Size-Dependent Transition to High-Symmetry Chiral Structures in AgCu, AgCo, AgNi, and AuNi Nanoalloys," *Nano Lett.,* vol. 10, no. 10, p. 4211–4216, 2010.
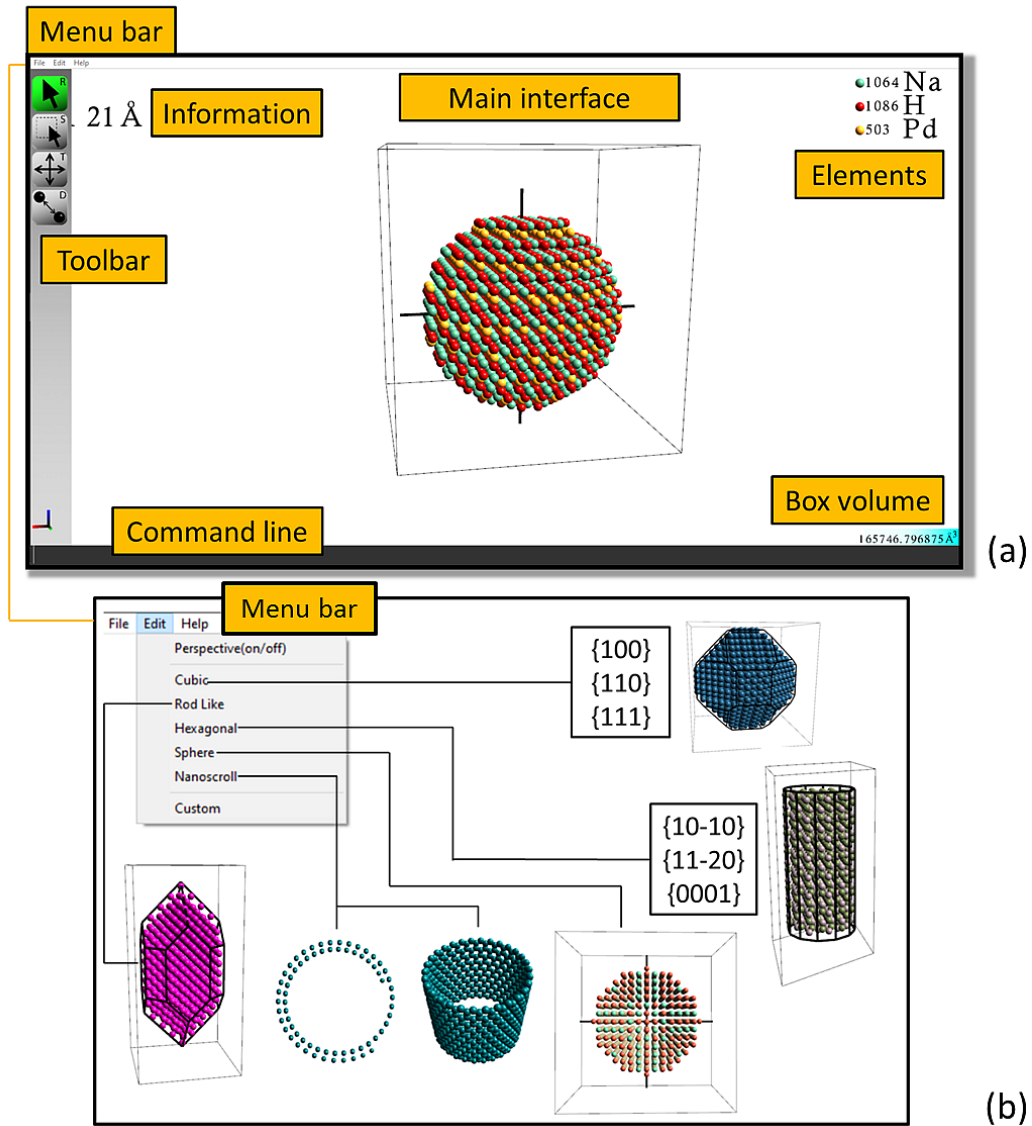
Figure 1: (a) The GUI of the NanoMaterialsCAD. (b) Current menu options for the creation of various nanostructures, referred to as "molds".
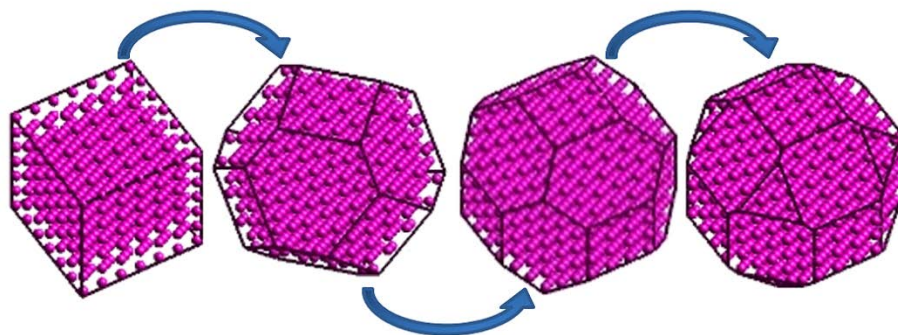
Figure 2: Smooth morphing via chamfering of a Cr NP from a cubic shape toward a truncated octahedron and a rhombicuboctahedron.
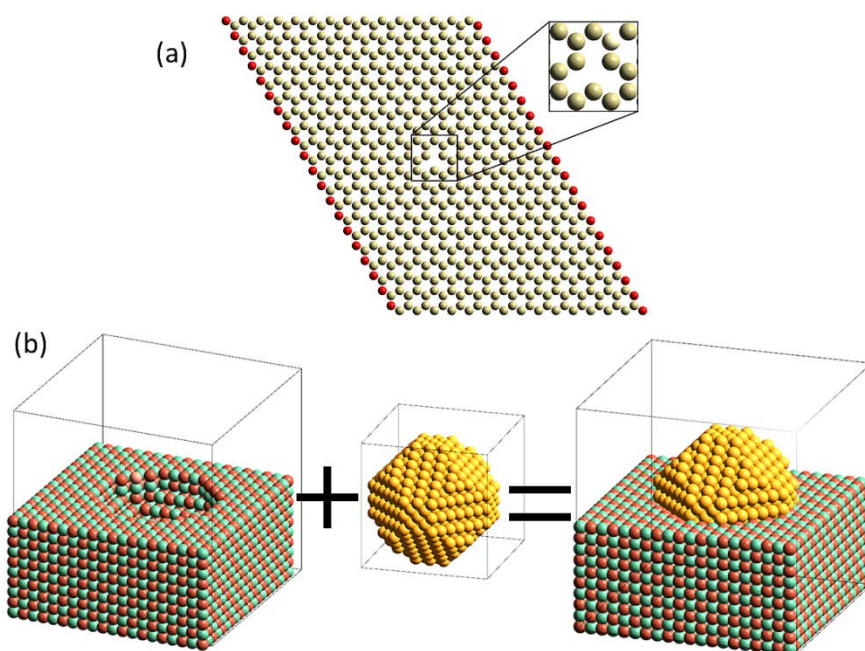

Figure 3: (a) Unrelaxed silicene nanoribbon terminated by H atoms (depicted red) with an added vacancy (magnified in inset). (b) Example of creation of semi-spherical hole on the (001) surface of a NaCl crystal, and deposition of a Pd NP, half-embedded in the support.
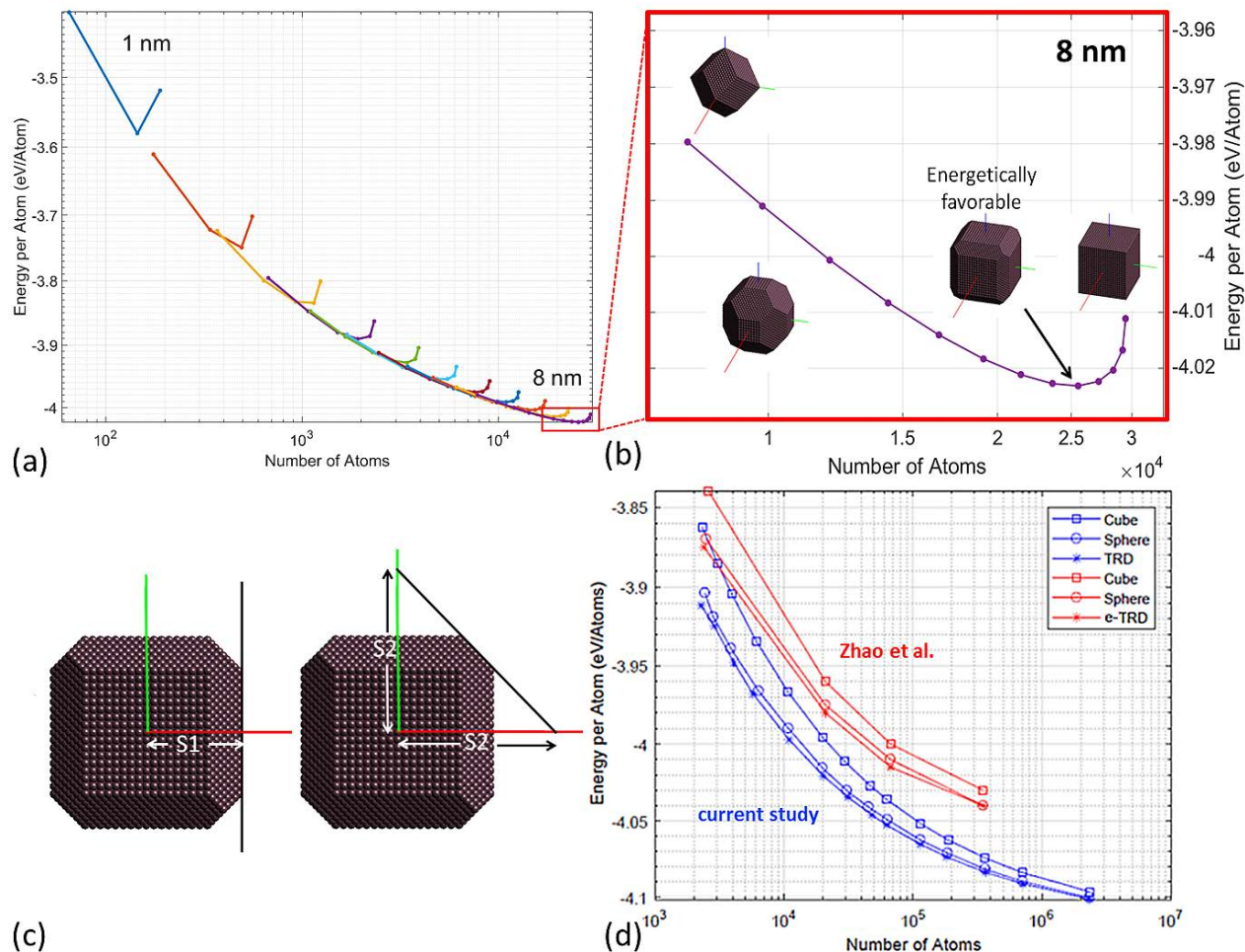
Figure 4: (a) Potential energy (in eV/atom) as a function of NP size (in number of atoms, to accommodate different NP shapes). Different chamfering sequences are marked by different colors. (b) Zoom-in at the chamfering sequence for 8 nm cubes, indicating the energetically favorable structure (i.e., a specific chamfered cube or non-equilateral TRD). (c) If S1 is the distance from the center of the NP to the intercept of a {100} facet on the x-axis, and S2 is the distance from the center of the NP to the intercepts of a {110} facet on the z and x axes, then as the ratio S2/S1 approaches the value 1.6 the energy of the NP approaches its minimum value, regardless of NP size. (d) Comparison between potential energy values as a function of size for three different shapes between the current work and Zhao et al. Note that for the latter work equilateral TRD results are shown, whereas for the former TRD corresponds to non-equilateral TRD.
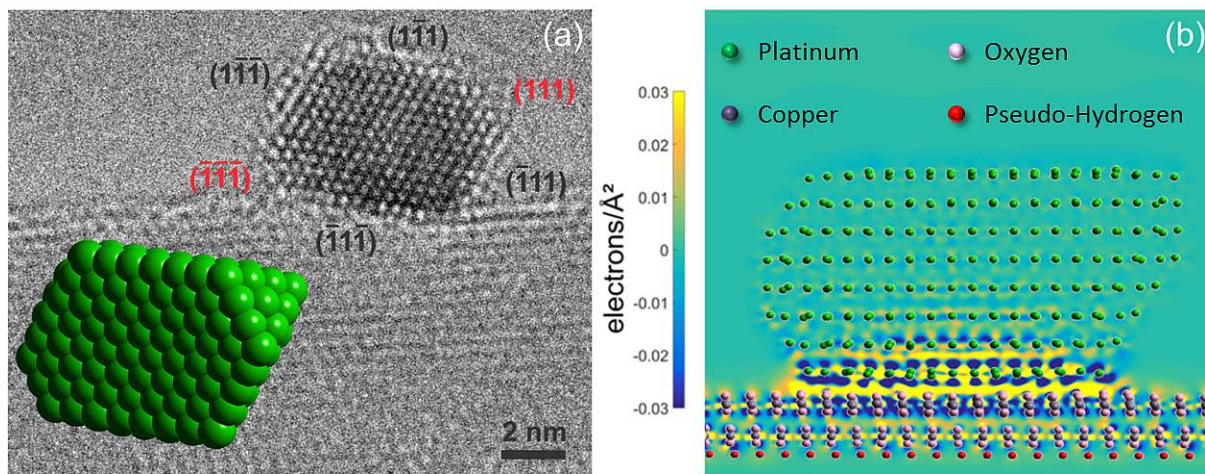
24

Figure 5: (a) HRTEM micrograph of Pt NP deposited on a CuO NW by magnetron-sputtering inert-gas condensation. The inset shows the reproduction of the NP by NanoMaterialsCAD, terminated by {111} surfaces only. The corresponding facet indices are denoted on the experimental image and it should be noted that along the specific [110] projection of the Pt structure the (111) and $(\overline{11}\overline{1})$ planes (in red font) are inclined with respect to the (110) plane, while the rest {111} facets of the NP are perpendicular. (b) Corresponding relaxed atomistic model of the system, showing its charge density transfer plot. Blue and yellow isosurfaces correspond to electron depletion and accumulation, respectively. Strong dipolar behavior is observed at the NP-support interface.
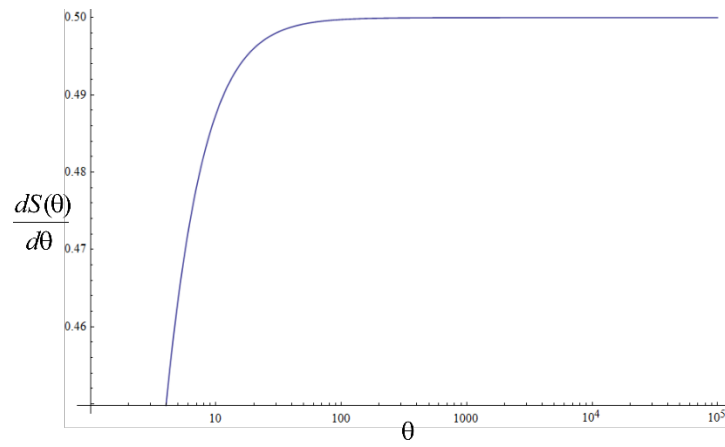
Figure A1: $\frac{dS(\theta)}{d\theta}$ vs. θ (in degrees) in a semi-log plot